Electron Capture Strength for ^{60,62}Ni and ^{58,60,62,64}Ni$(p,n)^{58,60,62,64}$Cu reactions at 134.3 MeV

N. Anantaraman,[1] Sam M. Austin,[2,3,*] B. A. Brown,[2,3] G. M. Crawley,[1,3] A. Galonsky,[1,3] R. G. T. Zegers,[2,3] B. D. Anderson,[4] A. R. Baldwin,[4] B. S. Flanders,[4] R. Madey,[4] J. W. Watson,[4] and C. C. Foster[5]

[1]*National Superconducting Cyclotron Laboratory Michigan State University, East Lansing Michigan 48824*
[2]*National Superconducting Cyclotron Laboratory and Joint Institute for Nuclear Astrophysics (JINA), Michigan State University, East Lansing, MI 48824*
[3]*Department of Physics and Astronomy, Michigan State University, East Lansing Michigan 48824*
[4]*Department of Physics, Kent State University, Kent Ohio 44242*
[5]*Indiana University Cyclotron Facility, Indiana University, Bloomington, Indiana 47405*

(Dated: May 15, 2008)

Background: The strength of electron capture for medium mass nuclei has a significant effect on the evolution of supernovae. There is insufficient knowledge of these strengths and very little data for important radioactive nuclei.
Purpose: Determine whether it is feasible to obtain EC strength from studies of T_o+1 excitations in (p,n) reactions, and whether this might yield information for radioactive nuclei.
Methods: Cross sections for the ^{58,60,62,64}Ni$(p,n)^{58,60,62,64}$Cu reactions were measured over the angular range of 0.3° to 11.6° at 134.3 MeV using the IUCF neutron time-of-flight facility.
Results: The T_o+1 excitations in ^{60,62}Ni were identified by comparison with inelastic proton scattering spectra, their B(GT) were extracted, and the corresponding electron capture rates in supernovae were calculated. Data from the TRIUMF (n,p) experiments at 198 MeV were reanalyzed; the electron capture rates for the reanalyzed data are in moderately good agreement with the higher resolution (p,n) results, but differ in detail. The possibility of future measurements with radioactive nuclei was considered.
Conclusions: It is possible to determine electron capture strength from (p,n) experiments. This approach may make it possible to obtain electron capture strength for radioactive nuclei by studying (p,n) reactions in inverse kinematics.

PACS numbers: 25.40.Kk, 95.30.Cq

I. INTRODUCTION

Interest in allowed Gamow-Teller strength in medium-mass nuclei ($A = 20-70$) is related to unresolved issues concerning weak strength in nuclear physics and astrophysics. The bulk of the electron capture (EC) strength in nuclei is not energetically accessible to direct measurement, but can be obtained from charge exchange reactions (CER): the CER cross section at low momentum transfer (small angles) is proportional to the Gamow Teller strength B(GT) for sufficiently high bombarding energies, above about 100-120 MeV/nucleon. The first systematic CER electron capture strength studies were performed at TRIUMF [1] using the (n,p) reaction at $E_n \approx 200$ MeV and achieved a resolution of about 1 MeV for a number of nuclei.

Large basis shell-model calculations for these nuclei [2] are in reasonably good agreement with the (n,p) data. There are, however, significant differences for the Ni isotopes [2, 3, 4]. More recent work with higher resolution, mostly with the (d, ^{2}He) reaction [5], has also been in general agreement with shell model calculations, but in some cases there are significant differences even in centroid locations [6]. Data from a recent ^{58}Ni(t,^{3}He)measurement [7] agree with the (d, ^{2}He) results [8] but less well with the TRIUMF data. The (t,^{3}He) data are in good agreement with shell model calculations using the KB3G two-body interaction at low excitation energies E_x, but the agreement is poorer at high E_x. The converse is true for the GXPF1 interaction(for a detailed discussion see Ref. [7] and references therein).

These uncertainties in predicted EC strength introduce uncertainties in predictions of the evolution of massive stars and the ensuing core-collapse supernovae. They also affect nucleosynthesis in Type Ia supernovae and the crust properties of neutron stars in accreting binary systems. For details see Ref. [9] and references therein. It appears that further experimental and theoretical work is necessary to better define the effective interactions used in shell-model calculations and to permit more reliable calculations of electron capture strength for astrophysical applications.

In this paper we describe a less direct approach to studying electron capture strength: obtaining β^+ strength from studies of charge exchange in the β^- direction. The strength of β^- transitions to T_o+1 states in the residual nucleus, where T_o is the isospin of the target nucleus, is related by an isospin geometry factor to

*Electronic address: austin@nscl.msu.edu; URL: www.nscl.msu.edu/~austin

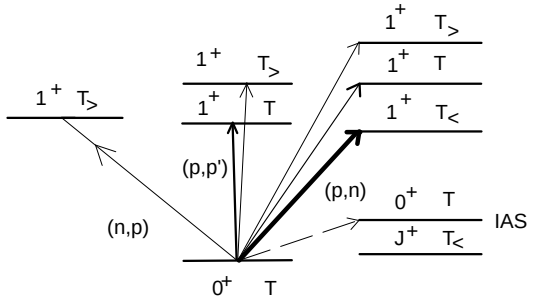

FIG. 1: Diagram of transitions via (p,n), (n,p) and (p,p') interactions. More intense transitions are shown by darker lines. With the exception of the transition to the isobaric analog state, those shown involve transfer of total angular momentum, spin, and isospin $\Delta J = \Delta S = \Delta T = 1$. States labelled with the same quantum numbers are isobaric analogs. The symbols $T_>$, T, and $T_<$ stand for $T_o + 1$, T_o and $T_o - 1$. We are concerned here with the relatively weak transitions to the $1^+, T_>$ states.

β^+ strength from the same nucleus, as shown in Fig. 1. Specifically, $\beta^+/\beta^- = (T_o + 1)(2T_o + 1)$. This method has been exploited previously for the obvious case of self-conjugate nuclei and for the $T = 1$ nuclei ^{26}Mg [10, 11] and ^{58}Ni [12, 13, 14]. Here we apply the technique to nuclei with higher isospin: ^{60,62,64}Ni.

To obtain $T_o + 1$ strength with (p,n) reactions, one has to deal with two important issues. First, the $T_o + 1$ states appear at high excitation energy, and lie on a large background; this is presumably the reason earlier experiments in this mass region with poorer statistics had not seen these states [15]. And second, charge exchange reactions such as (p,n) do not have an isospin meter; they are not selective of isospin. In the present high statistics (p,n) experiment on the $T = 2$ and $T = 3$ nuclei ^{60,62}Ni, we observe peaks at the expected energies of T_o+1 states and present reasonably convincing evidence that they are $T_o + 1$ states. It, therefore, appears that both of the above issues can be dealt with although some ambiguities remain.

In Section II we describe the experimental procedures and in Section III present the results for B(GT) and reaction rates. In Section IV we discuss some options for future measurements of electron capture strength for radioactive nuclei using inverse kinematics, with heavy radioactive beams incident on hydrogenous targets.

II. EXPERIMENTAL PROCEDURES

The beam-swinger time-of-flight system at the Indiana University Cyclotron Facility was used to measure neutron time of flight spectra resulting from the bombardment of 36 to 50 mg/cm^2 ^{58,60,62,64}Ni targets (isotopically enriched to $> 96\%$) by 134.3 MeV protons. The detection station was placed at 0°, 85.8 m from the target, and consisted of three identical, large volume, mean timed NE-102 detectors with a combined frontal area of 1.55 m^2 and a thickness of 10.16 cm [16]. Data were obtained at outgoing neutron angles of 0.3, 3.9, 8.0, and 11.6 deg for several different thresholds; all thresholds gave consistent results to within $\pm 5\%$. Efficiencies were calculated with the Monte Carlo code of Cecil *et al.* [17]. The overall energy resolution was about 500 keV FWHM, worse than usual, because of an unusual and uncorrectable jitter in the cyclotron timing signal. The total systematic uncertainty in the cross sections is $\pm 13\%$. The peaks of main interest, see Fig. 2, are those labelled $T_o + 1$, and located near $E_x = 14.4$ and 18.6 MeV in ^{60}Cu and ^{62}Cu, respectively. The state in ^{60}Cu was apparently not seen in lower statistics work on that nucleus at 120 and 160 MeV [15]. A more detailed view of the $T_o + 1$ cross sections is shown in panels (a) and (c) of Fig. 4. These results show that a high statistics experiment can observe the $T_o + 1$ states, even with relatively poor resolution.

III. RESULTS

The angular distributions for the high lying excitations in ^{60,62}Ni are shown in Fig. 3. The curves are DWBA calculated shapes for $L = 0$ performed with the code DWBA70 [19], effective interactions at 140 MeV from Love and Franey [20], optical model potentials of Ref. [21], and simple $(\pi f_{7/2} \nu f_{5/2}^{-1})$ wave functions. The observed angular distributions are forward peaked and are consistent with $L = 0$ GT excitations.

We next deal with the evidence for assigning $T_o + 1$ as the isospin of these peaks. Perhaps most important is the comparison with spectra for the (p,p') reaction that are shown on the energy axis in Fig. 2. The (p,p') reaction near zero degrees populates 1^+ states preferentially, with a spin strength proportional to B(GT) for the analog CER, but it can populate both isospin T_o and $T_o + 1$ states. The sharp states seen at high excitation in the (p,p') spectra have been assigned as $T_o + 1$ [18, 22] for two main reasons. First, as T_o of the target nucleus increases, these states shift systematically to higher E_x with respect to the T_o strength, as would be expected for a state of isospin T_o+1. And second, although the states are unbound to neutron decay and have low angular momentum, they are quite narrow; their observed width is consistent with the experimental resolution, presumably because the neutron decay of $T_o + 1$ states is isospin forbidden and the proton decay energy is well below the Coulomb barrier. The positions of the sharp (p,p') peaks agree approximately with those seen in (p,n), after correcting for Coulomb effects, supporting a $T_o + 1$ assignment for the states seen in the (p,n) reaction.

Shell model calculations done in a simple basis [23] also support the T_o+1 assignment; the T_o+1 strength is separated from T_o strength for $A > 58$, and is localized in a few strongly populated states. As expected, the separation grows as $N - Z$ increases. We shall see that

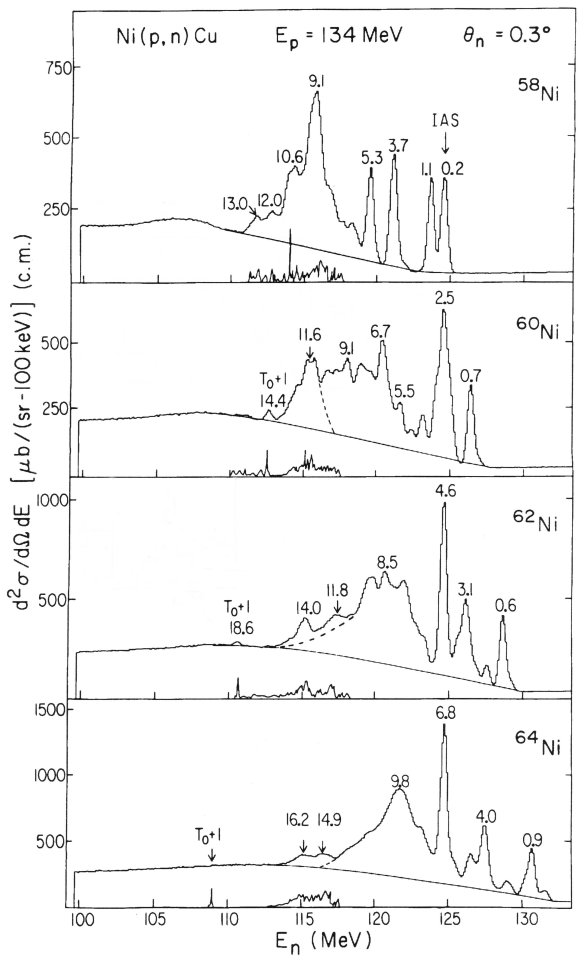

FIG. 2: Spectra for ^{58,60,62,64}Ni (p,n) reactions at 134.4 MeV. There are about 10^4 counts per channel in these spectra, sufficient to observe the weak T_o+1 states as described in the text. The numbers above the peaks in the spectra are excitation energies. Spectra observed in (p,p') reactions [18] on the target nuclei are plotted on the energy axis. The sharp peak at the left of each (p,p') spectrum is the lowest-lying T_o+1 state.

these states lie low in the spectra reached via (n,p) from the same target.

A. Comparison with (p,p')

The isospin analog of a state at E_x(target), seen in the (p,p') reaction, will occur in the (p,n) product nucleus at approximately the same energy above the analog of the ground state (labeled IAS in Fig. 1), i.e., $E_x(p,n) = E_x(p,p') + E_x(IAS)$. In Table I the relevant energies are tabulated, showing that the energies of the analogs of the strongly excited (p,p') states and of the observed peaks in ^{60,62}Cu agree within the accuracy of the present measurements (±0.1 MeV). There is also a small enhancement at the expected energy in ^{64}Cu (not visible

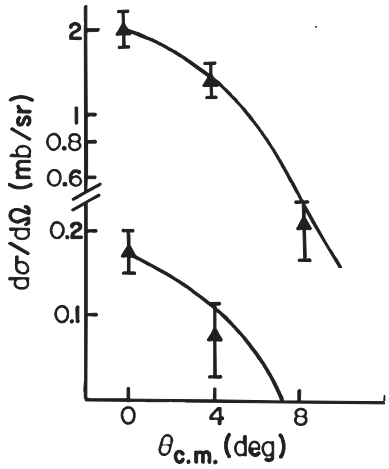

FIG. 3: Angular distributions for the T_o+1 excitations in ^{60}Ni (upper points) and ^{62}Ni (lower points). The ^{60}Ni cross sections have been multiplied by 10 for display purposes. The curves are the DWBA calculations described in the text.

on the scale of Fig. 2), but with the present resolution, it is barely one standard deviation above background, and is too weak to permit extraction of meaningful cross sections. The observed widths of the lowest lying T_o+1 peaks are consistent with the resolution of the (p,n) and (n,p) experiments (these states are isospin forbidden to decay by neutron emission and the proton decay energy for isospin allowed decays is in the 2 to 3 MeV range, well below the Coulomb barrier). The predicted excitation energies of the states in ^{A}Co that would be reached by the corresponding ^{A}Ni(n,p) transitions are also given in Table I.

B. Determination of B(GT)

We extracted the B(GT) corresponding to the T_o+1 excitations by comparing their strength to that of the Fermi ($\Delta L = \Delta S = 0$) transition to the IAS, (B(F) $\approx (N-Z)$), both evaluated at the same small momentum transfer ($q \approx 0.05$ fm^{-1}) using the standard techniques [25]. We make the usual assumption [25], fairly accurate for this energy range, that the ratio of cross sections for Fermi and GT transitions of equal strength is proportional to $(E_p(MeV)/54.9)^2$. This corresponds to a unit cross section, the ratio of cross section to B(GT), of 4.39 mb (4.23 mb) for ^{60}Ni (^{62}Ni), in good agreement with the value of 4.49 mb (4.29 mb) used by [4] at 198 MeV. This is not surprising since the energy dependence of unit cross sections is weak.

Determination of the number of counts in the T_o+1 states in ^{60,62}Ni was done by fitting the data with a polynomial background and a sum of Gaussians. The results for a quadratic background and two or three Gaussians are shown in Fig. 4. For ^{60}Ni a linear background did not adequately reproduce the overall spectrum shape. Fits to the ^{60}Ni data with three Gaussian peaks were

TABLE I: Expected and observed energies of the lowest lying $T_o + 1, 1^+$ states in the Cu isotopes following (p, n) reactions and in the Co isotopes following (n, p) reactions.

Target	$E_x(^A\text{Ni})^a$ (MeV)	$E_x(\text{IAS})^b$ (MeV)	$E_x(^A\text{Cu, expected})^c$ (MeV)	$E_x(^A\text{Cu, observed})$ (MeV)	$E_x(^A\text{Co, predicted})^d$ (MeV)	$E_x(^A\text{Co, observed})^e$ (MeV)
^{60}Ni	11.85 ± 0.02	2.54 ±0.02	14.39	14.4 ± 0.1	0.75	0.54
^{62}Ni	14.00 ± 0.02	4.63 ±0.01	18.63	18.6 ± 0.1	0.52	0.59
^{64}Ni	15.62 ± 0.02	6.82	22.4		0.25	

[a] From the ^{A}Ni (p, p') results of Refs. [18, 22]
[b] Ref. [24]
[c] From $E_x(p, n) = E_x(p, p') + E_x(IAS)$
[d] Calculated from $E_x(^A\text{Ni})$ in the first column and known Coulomb energies
[e] From fits to the data of Ref. [4] as shown in Fig. 4.

not superior within statistics, although they allowed for the use of the same width, consistent with the energy resolution, for the three peaks. For ^{62}Ni the lower lying peak was well defined, but the strength of a second peak could not be determined unambiguously; its area was fixed at the same value relative to the lower excitation peak as in the TRIUMF data (see below). This yields a satisfactory description of the data as shown in Fig. 4. The results for B(GT) are collected in columns (2) and (3) of Table II. The uncertainties shown include a 13% systematic error, dominated by the uncertainties in the cross section of the IAS (8%) and in the extrapolation to $q = 0$ (10%). In most cases the statistical uncertainty is larger, because the peaks sit on a large background. The B(GT) are converted to those that would be measured in (n, p) reactions by multiplying by the appropriate ratio of Clebsch-Gordon coefficients, 15 for ^{60}Ni and 28 for ^{62}Ni.

C. Comparisons with other (p, n) and (n, p)data

Data for ^{58,60}Ni are available from 120 MeV (p, n) measurements at IUCF [15], but the statistics are not sufficient to observe the weakly excited $T_o + 1$ states in ^{60}Ni. The 198 MeV Ni(n, p) reaction studies at TRIUMF observe the ^{58,60,62,64}Ni EC states directly [3, 4] and warrant a detailed comparison with the present data for ^{60,62}Ni. This is not possible for ^{58,64}Ni. The $T_o + 1$ strength in ^{58}Ni(p, n) is not sufficiently separated from T_o strength to permit a reliable identification without further information [12, 13, 14]. And as noted above the strength we observe for ^{64}Ni is significant only at the one standard deviation level.

Since only the stronger low-lying excitations can be extracted from the present data, in the 6th column of Table II we compare with the results from ref. [4] as reported in Fig. 12 of that paper, integrated over a comparable energy range, namely up to $E_x = 3.2$ or 4.0 MeV. The numbers quoted in Fig. 12 of Ref. [4] in this energy interval are about 25% smaller than those given in Fig. 10 and Table II of that paper, as has been previously noted in Ref. [2]; we use the results in Fig. 12 because they are given as a function of excitation energy.

A somewhat more detailed qualitative comparison is also possible. Figs. 2-4 of Ref. [4], referred to as "Williams" in the following discussion, present the (n, p) data prior to multipole decomposition. Those data are given in smaller bins than the final results, 300 keV compared to 1.0 MeV, and have structure that did not survive the multipole decomposition procedure. For example, the spectrum for ^{60}Ni in Fig. 2 of Williams has two peaks below $E_x = 4$ MeV that, as is shown by their Fig. 6, are dominated by $L = 0$ strength. These peaks are not separately visible in the $L = 0$ spectra of Williams, Fig. 9. We have scanned the Williams data (in their Figs. 2 and 3) for ^{60,62}Ni and fitted them with quadratic backgrounds and two or three Gaussians as was done for the 134.3 MeV data. For the Williams ^{60}Ni data, the three-Gaussian fits were superior. The quadratic backgrounds presumably account mainly for the contribution of higher L transitions, at least for the Williams data.

In Fig. 4 we show both the Williams cross section data at $E_n = 198$ MeV and the present data for the $T_o + 1$ states at $E_p = 134.3$ MeV. For ^{60}Ni, the locations and spacing of the two lowest states are in excellent agreement; for ^{62}Ni the position of the lowest lying state is the same within about 170 keV, consistent with combined experimental uncertainties. The cross sections for the lowest lying states near 0.6 MeV agree within the uncertainties. However, the relative intensities of the two lowest states for ^{60}Ni observed in the present 134.3 MeV data differ significantly from those in the Williams data. The reason for this difference is not understood. We have investigated whether changes in the details of the fitting procedure could significantly change this ratio; systematic changes in the ratio of more than 15% seem unlikely.

In order to convert the Williams cross section data of Fig. 4 to B(GT), the cross sections were extrapolated to 0° using the ^{64}Ni(n, p) angular distribution shown in Williams, Fig. 5, and then to $q = 0$ using the momentum transfer dependence found in the present 134.3 MeV data. The unit cross sections from Williams were used to convert the resulting cross sections to B(GT). The results are shown in Column 4 of Table II. Only statistical errors, typically 3-5% are quoted in Williams. It seems

TABLE II: Values of B(GT) for transitions to 1^+, $T_o + 1$ states in ^{A}Cu: (p,n); and in ^{A}Co: (n,p). The values are those for two-Gaussian fits, except for the TRIUMF (n,p) results for ^{60}Ni where the results for the three-Gaussian fits are shown in parentheses.

Target(E_x-MeV)[a]	B(GT)-(p,n)	B(GT)-(n,p)[b]	B(GT)-(n,p)[c]	$B(\mathrm{GT})_{sm}$[d]	$B(\mathrm{GT})_{TRIUMF}$[e]
^{60}Ni(0.65)	0.063 ± 0.010	0.95 ± 0.15	0.89 (1.03)		
^{60}Ni(2.4)	0.026 ± 0.008	0.39 ± 0.12	1.47 (0.97)		
^{60}Ni(0.65+2.4)	0.089 ± 0.014	1.34 ± 0.22	2.36 (2.00)	2.7 (3.0)	2.0
^{62}Ni(0.6)	0.032 ± 0.007	0.89 ± 0.20	1.01		
^{62}Ni(2.3)	0.014 ± 0.005	0.39 ± 0.14	0.40		
^{62}Ni(0.6+2.3)	0.046 ± 0.010	1.28 ± 0.29	1.41	1.9 (2.0)	1.3

[a]The E_x are the positions that these states would occur in the analog system ^{60}Co.
[b]Obtained by multiplying the results obtained from (p,n) listed in the second column by the isospin geometry factors: 15.0 for ^{60}Ni, and 28.0 for ^{62}Ni.
[c]From the data of Figs. 2 and 3 in Ref. [4] as analyzed in the present paper using, mainly, two-Gaussian fits. The values in parentheses for ^{60}Ni are the results of three-Gaussian fits after summing the strengths for the upper two states; for separate values see Fig. 5. For details see text.
[d]From Caurier, *et al.* [2]. The strength quoted is the sum of strengths to 1^+ states lying below 3.2 (4.0) MeV.
[e]From Ref. [4], Fig. 12, integrated over the energy range up to 3.2 (4.0) MeV.

probable, however, given various experimental uncertainties and uncertainties in the unit cross section that the overall uncertainties are at least 10% and perhaps larger.

As we have noted for the cross sections, the values of B(GT) from the (p,n) and (n,p) reactions agree within the uncertainties for the states near 0.6 MeV in ^{60,62}Ni, but the excitation of the 2.4 MeV state in ^{60}Ni is much stronger in (n,p).

D. Comparisons with shell-model calculations

In Table II we compare our results with the large basis shell-model calculations of Ref. [2]. These calculations use a renormalized (reduced) GT operator, $g_A/g_V = 1.0$ The theoretical strength is concentrated at low excitation, mostly below $E_x = 4.0$ MeV. However, we shall see later that the energy distribution of theoretical strength for ^{60}Ni differs greatly from experiment, mainly lying near the high energy peak of Fig. 4.

E. Comparisons of B(GT) and electron-capture rates

The values of B(GT) for ^{60}Ni from the two experiments and from the shell model calculations of Ref. [2] are shown in Fig. 5. In cases where the fitted cross section peaks had widths consistent with the experimental resolution we plotted their B(GT) at the position of the peak; this applied to the lower lying peak in all the data fitted in this paper and to the higher-lying peak when fitted by the sum of two Gaussians. When the higher-lying peak was fitted by a single Gaussian, the fitted width was greater than the resolution, and the strength was divided into 200 keV bins. The values obtained are plotted in panels (a) and (b) of Fig. 5. In Fig. 12 of Williams [4] the B(GT) are given in 1.0 MeV wide bins, with one of the bins extending to E_x = -0.5 MeV. The 1.0 MeV bins were subdivided into 200 keV intervals, and the values at $E_x < 0$ MeV were incorporated uniformly into the lowest three bins; the results are shown in panel (c). The shell model results of Ref. [2] are shown in panel (d).

There are significant differences among the distributions of B(GT) of Fig. 5. The results from Fig. 12 of Williams [4] extend to lower E_x than do those from the analyses of the same date carried out in this paper, presumably as a result of the binning procedure used in the multipole analysis. This will result in larger electron capture rates at relatively low temperatures and densities in astrophysical environments, as we show in Fig. 6. We would argue that the results of the present analysis are more reliable. On the other hand, the strengths predicted by the shell model [2] are peaked at high energies and will become important only at rather high temperatures or densities.

Electron capture rates are calculated for the different distributions of Fig. 5 using the code described in Ref. [26]. Electron chemical potentials were computed from a tabulation [27]. These calculations ignore contributions from higher-lying states and from capture on thermally excited states that will be important at high temperatures and densities. Details of the calculation and additional references are given in [7].

Rates were calculated on a grid including values of ρY_e from 10^1 to 10^{14} gcm^{-3} and of T from (0.01-100) $\times 10^9$ K. In Fig. 6 we show the rates for two representative ρY_e of interest in the pre-supernova evolution of massive stars: $\rho Y_e = 10^7$ and 10^9 gcm^{-3}. In a $25M_{sun}$ star, for example, the former is characteristic of various stages of Si burning, when the temperature $T_9 \approx 2-4$; the latter occurs late in the pre-supernova stage when $T_9 \gtrsim 10$. In panels (a) and (b) the absolute rates are shown: in panels (c) and (d) the rates are compared to those for the present 134.3 MeV data. For details, see the text.

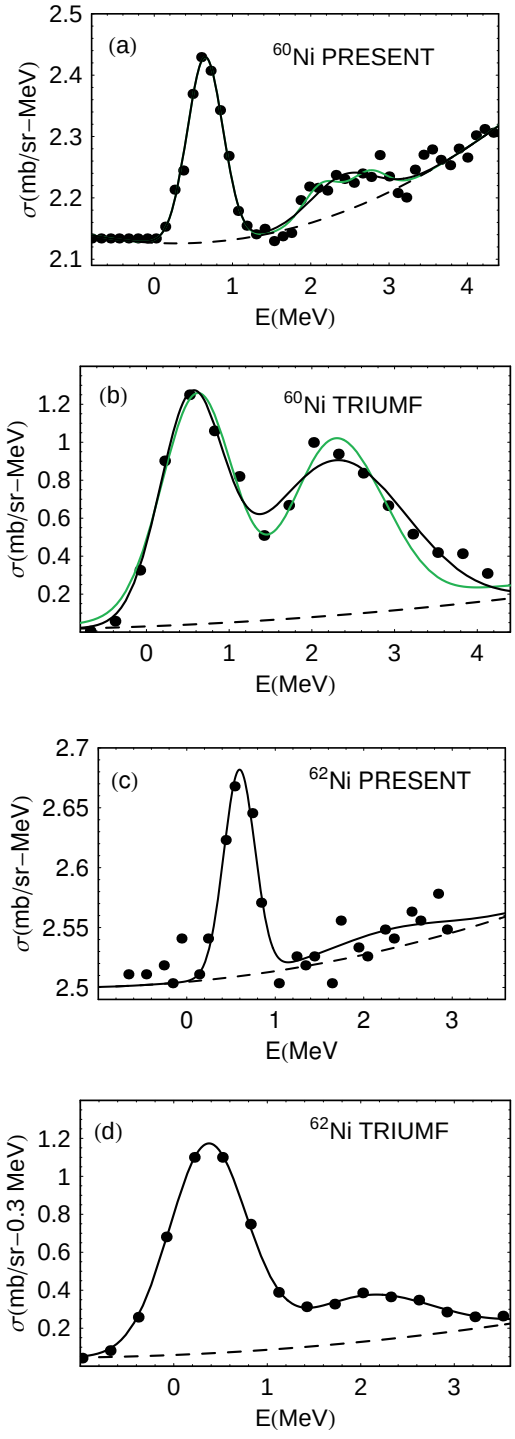

FIG. 4: (Color on line) Panel (a): Spectrum for ^{60}Ni$(p,n)^{60}$Co at 134.3 MeV, in the region of the T_o+1 states. The black and gray curves are two- and three-Gaussian fits, resp. Panel (b): Spectrum for ^{60}Ni$(n,p)^{60}$Co at 198 MeV. The black and gray curves are two- and three-Gaussian fits, resp. Panel (c): Spectrum for ^{62}Ni$(p,n)^{62}$Co at 134.3 MeV, in the region of the T_o+1 states. Panel (d): Spectrum for ^{62}Ni$(n,p)^{62}$Co at 198 MeV. The 198 MeV data are from Ref. [4] and the 134.3 MeV data are from the present work. Spectra are fitted with a second order polynomial background and two or three Gaussian peaks. For details see the text.

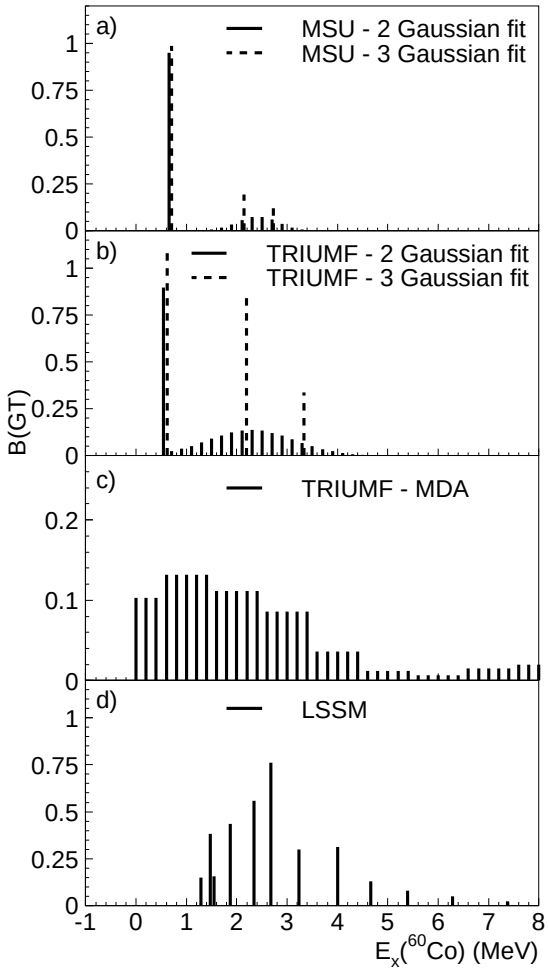

FIG. 5: Values of B(GT) for ^{60}Ni obtained from the present 134.3 MeV (p,n) data and the 198 MeV TRIUMF (n,p) data. Panels (a) and (b) show the results of the fits to the (p,n) and the (n,p) cross sections as described in the text and shown in Fig, 4. Panel (c) shows B(GT) from the Multipole Decomposition Analysis (MDA) performed in Williams [4], and shown in Williams Fig. 12. The results from large scale shell model calculations [2] are shown in panel (d). For details see the text.

We find that: (1) The rates for the two- and three-Gaussian fits to the 134.3 MeV (p,n) data are almost the same over the entire parameter space, reflecting the similarity of the two and three-Gaussian fits. (2) The TRIUMF results for the Gaussian fits made in the present paper differ from the 134.3 MeV data, but rates for the three-Gaussian fits are in fairly good agreement, especially at the higher densities and/or temperatures. (3) At lower temperatures and densities, the rates for the B(GT) results presented in Fig. 12 of Williams [4] are considerably higher than the others shown.

We conclude from these comments that the Multipole Decomposition Analysis for the TRIUMF data affects the resulting B(GT)s significantly, at least for ^{60}Ni. It also appears that obtaining electron capture rates from (p,n)

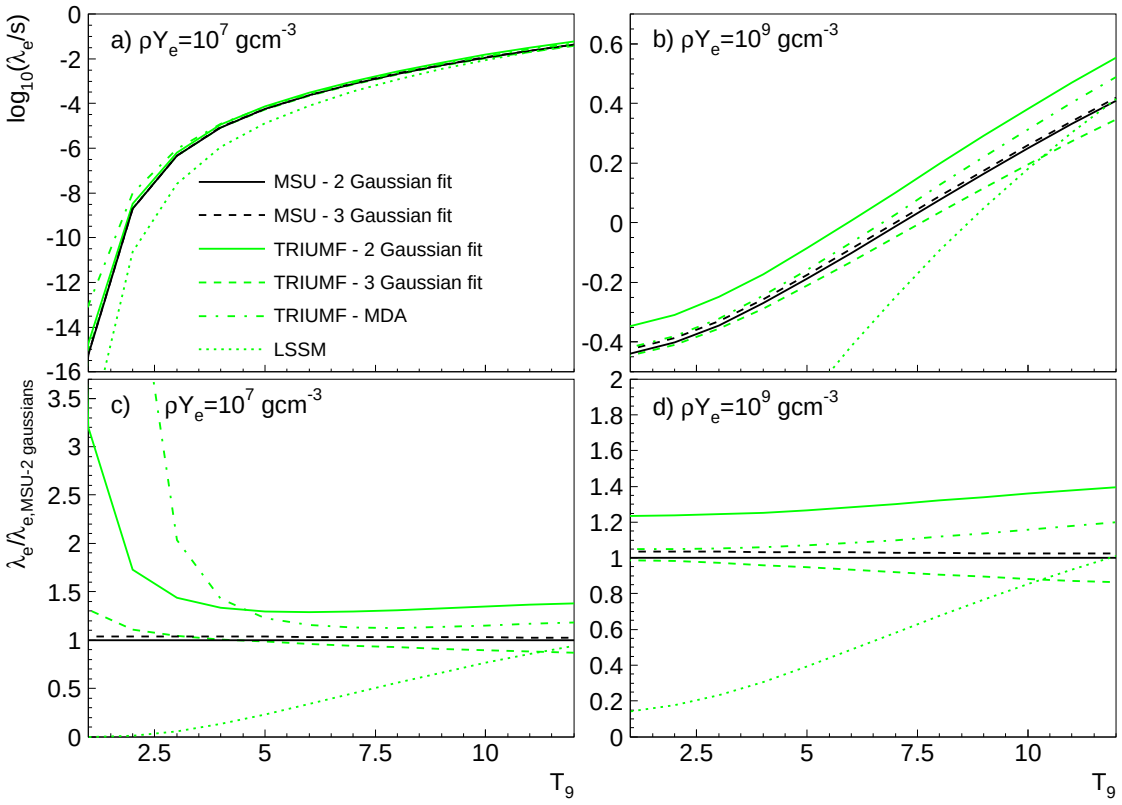

FIG. 6: (Color on line)Reaction rates obtained from the B(GT) of Fig. 5. The upper two panes show the absolute rates and the lower two panels the results compared to those for the 134.3 MeV (p,n) data. For details see the text.

data is a viable procedure.

IV. MEASUREMENTS OF EC STRENGTH FOR RADIOACTIVE NUCLEI.

Studies of the electron capture strength of radioactive nuclei must be done using inverse kinematics (IK), with a radioactive beam of heavy nuclei incident on a light target. Such studies will be necessary to explore nuclei with significant neutron excesses and to make possible studies on odd-odd nuclei; among these only ^{50}V is a stable target. Under the conditions of interest ($\theta_{c.m.}$ near 0°, E_x in the 0-15 MeV range) the outgoing light particles typically have small energies; if these particles are charged, exceedingly thin targets are required, yielding a very small reaction rate. The (p,n) reaction does not have this problem; the low energy neutrons can easily leave the target.

There are, however, limitations on the use of the (p,n) technique. It is applicable only to nuclei with isospin large enough that the splitting of T_o and T_o+1 states allows one to isolate T_o+1 strength with reasonable certainty. For a $T_o=1$ nucleus like ^{58}Ni the T_o and T_o+1 excitations are strongly intermixed as discussed in detail in ref. [12]. Because the strength of a transition is roughly proportional to $1/T_o^2$, the isospin must also be sufficiently small that the T_o+1 states are observable. In the present experiment the T_o+1 states were barely seen in ^{64}Ni with $T_o=4$. Better resolution would increase the peak to background ratio and make it possible to observe T_o+1 states for nuclei with higher isospin. If, for example, a resolution of 200 keV could be obtained for IK (p,n) reactions, 2.5 times better than in the present experiment, one could study nuclei where the relative strength of the T_o+1 excitations is a factor of 2.5 smaller, corresponding to T_o as large as 5 (^{62}Ni has $T_o=3$). It is not clear whether such nuclei can be reached in practice; one may be limited by the intrinsic decay widths or spreading widths of the states. And obtaining 200 keV resolution will be challenging; it will certainly require the intensities of an advanced radioactive beam facility. At present intensities feasible resolutions are in the 0.5-1.0 MeV range.

Inverse kinematics (p,n) approaches are being undertaken at the NSCL. Detecting the low energy neutrons is feasible, but presents a significant challenge. Moreover, the c.m. energy typically depends on the laboratory angle of the emitted neutron so the detection system must have high angular granularity to obtain good resolution

in E_x. Construction of a detector that will meet these challenges is underway.

V. SUMMARY

We have shown that (p,n) reactions at 134.3 MeV have sufficient sensitivity to extract B(GT) for strongly excited T_o+1 states, provided that the isospin of the target nucleus is neither too large nor too small. Electron capture strengths for the lowest lying T_o+1 states in ^{60,62}Ni were extracted from data for the (p,n) reaction and compared with (n,p) data and with large basis shell model predictions. The fits to the raw TRIUMF (n,p) cross section data performed in the present paper yield results rather close to the (p,n) results for the lowest lying peak but have larger strength to higher-lying states for ^{60}Ni as shown in Fig. 4. However, the multipole analysis leading to the B(GT) presented in Williams Ref. [4] moves some strength to lower energies.

Electron capture rates were calculated for two cases of interest in the pre-supernova evolution of massive stars. The results for the present analyses of the 134.3 MeV (p,n) data and of the Williams (n,p) data are in reasonable agreement, except at the lowest temperatures and densities. However, the B(GT) extracted by the Williams multipole analysis yields significantly larger rates, particularly at low T.

That (p,n) reactions lead to electron capture rates that are in agreement with (n,p) results, when both are analyzed in the same fashion, supports using (p,n) reactions in IK to study T_o+1 states in radioactive nuclei. We conclude that the IK approach may be useful for the radioactive nuclei that play an important role in supernova evolution and whose electron capture strength is difficult to obtain in other ways.

Acknowledgments

The authors wish to thank Parker Alford, Y. Fujita, M. Fujiwara, and Grant Mathews for useful conversations and comments. This work was supported in part by the National Science Foundation.

[1] W. P. Alford and B. M. Spicer, Adv. Nucl. Phys. **24**, 1 (1998).
[2] E. Caurier, K. Langanke, G. Martínez-Pinedo, and F. Nowacki, Nucl. Phys. **A653**, 439(1999).
[3] S. El-Kateb, *et al.*, Phys. Rev. C **49**, 3128 (1994).
[4] A. L. Williams, *et al.*, Phys. Rev. C **51**, 1144 (1995).
[5] D. Frekers, Nucl. Phys. **A731**, 76 (2004).
[6] D. Frekers, Nucl. Phys. **A752**, 580c (2005).
[7] A. L. Cole, *et al.*, Phys. Rev. C **74**, 034333 (2006).
[8] M. Hagemann, *et al.*, Phys. Rev. C **71**, 014606 (2005).
[9] K. Langanke and G. Martínez-Pinedo, Rev. Mod. Phys. **75**, 819 (2003).
[10] R. Madey, B. S. Flanders, B. D. Anderson, A. R. Baldin, C. Lebo, J. W. Watson, Sam M. Austin, A. Galonsky, B. H. Wildenthal, and C. C. Foster, Phys. Rev. C **35**, 2011 (1987) and **36**, 1647 (1987).
[11] R. G. T. Zegers, *et al.*, Phys. Rev. C **74**, 024309 (2006).
[12] Y. Fujita, *et al.*, Phys. Lett. **B365**, 29 (1996).
[13] Y. Fujita, *et al.*, Eur. J. Phys. **13**, 411 (2002).
[14] H. Fujita, *et al.*, Phys. Rev. C **75**, 034310 (2007).
[15] J. Rapaport, *et al.*, Nucl. Phys. **A410**, 371 (1983).
[16] R. Madey, *et al.*, Nucl. Instrum. Methods Physics Research **214**, 401 (1983).
[17] R. A. Cecil, B. D. Anderson, and R. Madey, Nucl. Instrum. Methods **161**, 439 (1979).
[18] N. Marty, C. Djalali, M. Morlet, A. Willis, J. C. Jourdain, N. Anantaraman, G. M. Crawley, and A. Galonsky, Nucl. Phys. **A396**, 145c (1983).
[19] J. Raynal and R. Schaeffer, CEN Saclay (unpublished.).
[20] W. G. Love and M. A. Franey, Phys. Rev. C **24**, 1073 (1981).
[21] V. Comparat, R. Frascaria, N. Marty, M. Morlet, and A. Willis, Nucl. Phys. **A221**, 403 (1974).
[22] C. Djalali, N. Marty, M. Morlet, A. Willis, J. C. Jourdain, N. Anantaraman, G. M. Crawley, A. Galonsky, and P. Kitching, Nucl. Phys. **A388**, 1 (1982).
[23] B. A. Brown, unpublished.
[24] M. S. Antony, J. Britz, and A. Pape, At. Data Nucl. Data Tables **40**, 9 (1988).
[25] T. N. Taddeucci, C. A. Goulding, T. A. Carey, R. C. Byrd, C. D. Goodman, C. Gaarde, J. Larsen, D. Horen, J. Rapaport, and E. Sugarbaker, Nucl. Phys. **A469**, 125 (1987).
[26] A. D. Becerril Reyes, S. Gupta, K. L. Fratz, P. Moller and H. Schatz, in Proc. International Symposium on Nuclear Astrophysics IX, Geneva, POS(NIC-IX)075 (2006).
[27] F. X. Timmes and F. D. Swesty, Astrophys. J. Supp. **126**, 501 (2000).